Research in Veterinary Science 109 (2016) 121–128

Contents lists available at ScienceDirect

Research in Veterinary Science

journal homepage: www.elsevier.com/locate/rvsc

Microvascular lesions and changes in cell proliferation and death, and cytokine expression in the placentas of mice experimentally infected with *Equid Herpesvirus 1*

C.N. Zanuzzi [b,e,*,1], M.E. Bravi [a,g,1], M.R. Scrochi [a,b,e], F. Nishida [c], N.A. Fuentealba [a,e], M.E. Diessler [b], H.G. Sguazza [a], C.I. Muglia [d,e], E.J. Gimeno [e], E.L. Portiansky [c,e], C.G. Barbeito [b,c,e], C.M. Galosi [a,f]

[a] Department of Virology, School of Veterinary Sciences, National University of La Plata, Argentina
[b] Department of Histology and Embryology, School of Veterinary Sciences, National University of La Plata, Argentina
[c] Image Analysis Laboratory, School of Veterinary Sciences, National University of La Plata, Argentina
[d] Department of Immunopathology, Institute of Immunological and Physiopathological Studies (IIFP), Argentina
[e] National Research Council (CONICET), Argentina
[f] Scientific Research Commission (CIC) of Province of Buenos Aires, Buenos Aires, Argentina
[g] Agency for the Promotion of Science and Technology (ANPCyT), Argentina

ARTICLE INFO

Article history:
Received 5 April 2016
Received in revised form 23 August 2016
Accepted 12 September 2016
Available online xxxx

Keywords:
Equid Herpesvirus 1
Proliferation
Apoptosis
Cytokines
Mice
Abortion

ABSTRACT

This study describes the changes observed in the placentas of mice experimentally infected with an abortigenic strain of EHV-1 at mid-pregnancy and euthanized at days 3 and 4 post-infection. We analyzed microscopic vascular alterations, cell proliferation and death by immunohistochemistry, and the expression of IFN-γ, TNF-α and the IL-10 by qPCR and flow cytometry. Infected mice showed slight respiratory signs and ruffled fur during the first two days post-infection. Virus isolation and DNA detection were positive only in the lungs of the infected mice. Vascular congestion, increase in the labyrinth area, and a significant reduction in fetal capillary endothelium surface of infected placentas were found. Cell proliferation was significantly reduced in the infected placentas, whereas the apoptosis was significantly increased. IL10, TNF and IFN-γ showed different expression in the infected placentas and uteri. The effects of EHV-1 during pregnancy depend on different pathogenic mechanisms in which vascular alterations, and cell death and proliferation and local cytokine changes are compromised.

1. Introduction

Equid Herpesvirus 1 (EHV-1) is an alphaherpesvirus that causes respiratory disease, abortion, perinatal mortality and neurological disorders in horses (Lunn et al., 2009). Most of the effects observed in the natural host were also validated in the murine experimental model. The model has been elicited to further investigate viral behavior in the host, the host immune response, the vaccine potential of several immunogens (Ruitenberg et al., 1999; Walker et al., 1999a; Zhang et al., 2000, Fuentealba et al., 2014; Zanuzzi et al., 2014) and the effect of antiviral agents (de la Fuente et al., 1992) using EHV-1 strains of different pathogenicity (Awan et al., 1995; van Woensel et al., 1995; Osterrieder et al., 1996; Walker et al., 1999b; Fitzmaurice et al., 1997). Our interest relies on the not yet fully elucidated pathogenic mechanisms of the reproductive failures. Major advances in this topic were obtained from studies carried out in mares, mainly focused on vascular changes to explain the reproductive failures caused by highly virulent endotheliotrophic strains (Allen and Bryans, 1986; Walker et al., 1999b; Lunn et al., 2009).

Several mechanisms were described in the pathogenesis of embryonic death and abortion of different reproductive diseases, such as changes in cell proliferation and programmed cell death, and in the systemic and local immune responses. Uterine natural killer (uNK) cells are involved in the development of normal placenta but also implicated in pathologic pregnancies (Bilinski et al., 2008; Murphy et al., 2009; Lash and Bulmer, 2011; Bulmer and Lash, 2015). Changes in the expression of carbohydrates and some cytokines have also been specifically

* Corresponding author at: Facultad de Ciencias Veterinarias, UNLP, Calles 60 y 118, 1900 La Plata, Argentina.
E-mail address: carozanuzzi@gmail.com (C.N. Zanuzzi).
[1] María Emilia Bravi shares first authorship with Carolina Zanuzzi.

http://dx.doi.org/10.1016/j.rvsc.2016.09.005
0034-5288/

associated with spontaneous and infectious induced abortions (Woudwyk et al., 2012, 2013).

Despite considerable research, the pathogenic mechanism by which EHV-1 induces abortions both in the natural host and the murine model remains unexplained. Since abortion is a multifactorial event we studied vascular and morphological changes, cell proliferation and death, and compared the expression of three cytokines of great relevance during pregnancy and viral infection: IFN-γ, TNF-α and IL-10 in uteri and placentas of mice experimentally infected with an abortigenic strain of EHV-1, at mid-pregnancy.

2. Materials and methods

2.1. Virus strain culture

The Argentinean AR8-EHV-1 strain was selected from the virus collection at the Department of Virology (School of Veterinary Sciences, National University of La Plata). This strain was isolated in our laboratory in 1996 from a sample of a fetus aborted in a rainstorm of abortions occurred in 1995 on an Argentinian farm (unpublished data). A genomic study of this strain showed no changes in comparison to the well-known abortigenic strains Ab4 and V592 (Fuentealba et al., 2011). After 4 passages in RK13 (rabbit kidney) cells grown in minimal essential medium (MEM) supplemented with 10% fetal calf serum (FCS), a viral stock was titrated by the standard Reed and Muench method, aliquoted and stored at −70 °C until used.

2.2. Mating protocol

Twenty-five-weeks-old specific pathogen-free female BALB/c mice were provided by the Department of Laboratory Animals (School of Veterinary Sciences, National University of La Plata, Buenos Aires, Argentina) and kept in conventional animal rooms. Temperature, light and ventilation were controlled, and animals received food and water *ad libitum*. After one week acclimation their estrous cycle was synchronized using the Whitten effect (Whitten, 1966). Once receptive, a group of females were caged with males at a ratio of 3:1 and pregnancies were confirmed by the presence of vaginal plugs (day 1 of pregnancy). Pregnant mice were then individually caged. The assays were sequentially developed according to availability of pregnant females.

Mice were weighted before mating and at day 13 after mating. Current proceedings were revised and approved by the Institutional Animal Care and Use Committee of the School of Veterinary Sciences (CICUAL), National University of La Plata (CICUAL-Res. T35-6-13) and performed in accordance with the Guide for the Care and Use of Laboratory Animals of the National Research Council.

2.3. Experimental design, collection and processing of samples

At day 13 of pregnancy mice were intranasally inoculated with 50 μl (20,000 $CCID_{50}$) of culture supernatant of AR8-infected RK13 cells (infected groups) or 50 μl of virus-free cell culture (control groups), under light anesthesia with isoflurane (Baxter Co., Deerfield, IL, USA). After virus inoculation, mice were checked daily to evaluate the general condition and to recognize the onset of clinical signs. All mice were deeply anesthetized and killed by exsanguination either at day 3 (infected group -ID3- $n = 5$, and its corresponding control group -CD3-, n = 5), or day 4 (infected group -ID4-, n = 5 and its corresponding control group -CD4-, n = 5) post-infection (pi) (Fig. 1).

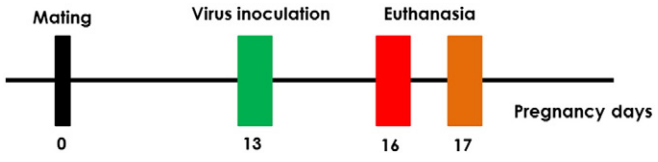

Fig. 1. Schedule of experimental design. Infection and euthanasia days.

At necropsy samples of lung, liver, uterus, placenta and fetus from control and infected groups were collected and processed for histological, immune or lectinhistochemical studies, virus isolation, PCR or cytokine determinations. Placentas were longitudinally cut in two equal parts along their major axis to be processed for histopathological or molecular studies.

2.4. Virus isolation

To corroborate the infection samples of lung, liver, spleen, placenta and fetus from all euthanized animals were processed for virus isolation by preparing a 10% (wt/vol) homogenized suspension in MEM with 2% of FCS (M-MEM) and clarified by centrifugation at 6000 *g* for 20 min. The supernatants were spread over RK13 cells and daily observed for cytopathic effect for one week. Samples without evidence of cytophatic effect were re-passaged twice before being considered as negative.

2.5. PCR studies

Samples of homogenates of control and infected groups that were used for viral isolation, and cells inoculated with a third passage of samples that were negative for virus isolation were processed for DNA extraction using a commercial kit (Wizard Genomic DNA Purification Kit, Promega, Madison, USA). PCR was performed using a pair of specific oligonucleotide primers that amplified a 369-bp fragment derived from a conserved gC region of EHV-1:

5′-CAACAATCGGGGAGGCGTCATA-3′(position 21,582–21,603) and.

5′-GTAGCATAGACTGGTACAGGGA-3′ (position 21,929–21,950).

DNA amplification was conducted as described elsewhere (Galosi et al., 2001).

2.6. Cytokine determination

Homogenates of uteri and placentas obtained both from control or infected groups were treated with protease inhibitor and used to determine a cytokine mRNA profile. Total RNA was then extracted with 1 ml of TRIzol (Invitrogen) per 100 mg of disaggregated tissue. cDNA synthesis was performed with M-MLV (Promega) according to the manufacturer's protocol. The relative amount of each cytokine (TNF-α, IFN-γ and IL-10) was measured by Real-time RT-PCR (q-PCR) using specific primers. Amplification was conducted following a previously standardized protocol (Woudwyk et al., 2012), using SYBR® Green (Applied Biosystems, USA) and carried out in an iCycler (Bio-Rad, USA). All samples were normalized in relation to their β-actin mRNA content. The relative quantification of the cytokines studied was expressed as $2^{-\Delta\Delta Ct}$.

In addition, the expression of TNF-α, IFN-γ and IL-10 proteins in uteri and placentas was analyzed by flow cytometry using the CBA TH1-TH2-TH17 system (BD Biosciences) in a FACS Calibur cytometer.

2.7. Histological, immune and lectinhistochemical studies

All samples were fixed in 10% neutral buffered formaldehyde (pH 7.4) for 24 h and then dehydrated, clarified, and embedded in paraffin wax.

2.7.1. Histological and histochemical studies

Sections of 3 μm of each sample were stained with hematoxylin and eosin (HE). Periodic Acid Schiff (PAS) technique (Bancroft and Stevens, 1990) was also applied to placentas to recognize uNK cells (Kusakabe et al., 1999). Morphological descriptions and morphometric measurements were conducted by researchers who were unaware of the groups being analyzed.

2.7.2. Immunohistochemistry (IHC)

Sections of 3 μm of each sample were mounted on positively charged slides (Biotraza microscope slides, Cat. #HDAS001A, Huida Medical Instruments Co., Jiangsu, China). Sections were deparaffinized, rehydrated, incubated with 3% H_2O_2 to inhibit endogenous peroxidase in methanol for 30 min at room temperature, and rinsed in phosphate-buffered saline (PBS, pH 7.4). Antigen retrieval was applied using 800 W of microwave irradiation twice for 3 min in citrate buffer, pH 6.0. Nonspecific binding sites were blocked with 2% bovine serum albumin (BSA) and 5% skim milk (for EHV-1 antigen) or 1% BSA (for PCNA antigens) for 30 min in a humid chamber at 4 °C. All primary antibodies were incubated for 1 h at 37 °C. Detection of viral antigens in lungs, livers, spleens, uteri, fetuses and placentas was performed using a primary polyclonal anti-EHV-1 rabbit serum produced in our laboratory (1/1600 dilution), followed by the secondary anti-rabbit EnVision detection system HRP (DakoCytomation). As a negative control, the primary antibody was replaced with normal rabbit serum. Proliferation process was evaluated in the placentas using the mouse monoclonal anti-PCNA antibody (clone PC 10, ascites fluid, Sigma Chemical Co., St. Louis, MO, EE. UU, 1/3000 dilution), previously pretreated with Dako ARK (Animal Research Kit) Peroxidase System (code K3954) to reduce the possible reactivity of the detection system with endogenous immunoglobulin. Nonspecific binding sites of endogenous biotin were blocked with an avidin–biotin blocking kit (Cat.#HK102-5K, Biogenex, Fremont, CA). Primary antibody was replaced by normal mouse serum as a negative control of the reaction. For both techniques liquid 3,3-diaminobenzidine tetrahydrochloride (DAB) was used as chromogen (DakoCytomation, Glostrup, Denmark), and Hill's hematoxylin was used for counterstaining.

2.7.3. Terminal deoxynucleotidyltransferase UTP nick end labeling (TUNEL) technique

This technique was used to study apoptosis, using the TUNEL In situ Cell Death Detection Kit, TMR red (Roche). Briefly, sections were deparaffinized, dehydrated and incubated with proteinase K for antigen retrieval. After washing with PBS containing 0.5% Tween 20 (Merck, Schuchardt OHG, Hohenbrunn, Germany) slides were incubated with the reaction mixture containing modified nucleotides (TMR-dUTP) and the enzyme terminal deoxynucleotidyltransferase (TdT) that catalyzes the template-independent polymerization of deoxyribonucleotides to the 3′-end of single- and double-stranded DNA. After washing, nuclei were counterstained with 5 μg/ml of DAPI (6-diamidino-2-phenylindole — Invitrogen Life Technologies, Eugene, Oregon, USA) following the manufacturer's protocol. Coverslips were mounted on slides using the aqueous medium Reagent FluoroSave™ (Calbiochem, La Jolla, CA, USA) and then examined under confocal microscopy. The TUNEL reaction mixture replaced by the label solution of the kit was used as a negative control of the reaction.

2.7.4. Lectinhistochemistry

To study vascular changes in the placentas of infected mice the BSA-1 lectin (*Bandeiraea simplicifolia/Griffonia simplicifolia*, with affinity for terminal α-D-galactosyl residues and N-acetyl-α-D-galactosaminyl residues) was analyzed, since it is used as a marker of fetal capillary endothelium of placental labyrinth during mid-late gestation; this lectin distinguishes the endothelial cell layer of fetal capillaries from maternal blood spaces (in which endothelial cell layer is absent) (Charalambous et al., 2013; Motta et al., 2015). Distribution of this lectin binding staining on control and infected placentas was compared. Sections were deparaffinized in xylene and rehydrated through an ethanol series to PBS. Endogenous peroxidase activity was blocked using hydrogen peroxide. To increase the exposure of carbohydrate residues microwave irradiation was applied at 800 W two folds for 3 min each in citrate buffer, pH 6.0. BSA-1 lectin (Lectin Kit BK 1000, Vector Laboratories, Inc., Burlingame, CA, USA) was incubated for 1 h at 37 °C. The horseradish peroxidase streptavidin SA-5704 (Vector Laboratories, Inc., Burlingame, CA, USA) was used as a detection system and incubated for 30 min at room temperature. Slides were then rinsed three folds in PBS for 5 min each time. Liquid 3,3′-diaminobenzidine tetrahydrochloride (DAB) was used as chromogen (Vector Laboratories, Inc., Burlingame, CA, USA). Negative controls for lectin staining included sections exposed to horseradish peroxidase and substrate medium without lectin. The dark, golden brown DAB-H_2O_2 reaction product showed the positively stained structures. Hill's hematoxylin was used for counterstaining.

2.8. Morphometry, cell proliferation and death quantification

Quantification of cell proliferation and death quantification was performed using CellSens Dimension (v1.6. Olympus Co., Japan) and Image-Pro Plus 6.3 (Media Cybernetics, Bethesda, MD) image analysis software.

2.8.1. Morphometry

To determine the extension of the labyrinth and spongiotrophoblast areas the whole HE stained sections were used. The giant cell layer was also included in the analysis. Images were captured using a 4× objective.

2.8.2. Proliferation and death quantification

Positive nuclei for PCNA and TUNEL in 10 captured images using a 20× objective were counted using the automatic Histogram Based function of the image analyzer. Percentages of positive nuclei over the total nuclei count were calculated.

2.8.3. Quantification of BSA-I lectin labeling

To isolate the BSA-I chromogenic signal from the rest of the tissue a color based segmentation was performed per image. As a result, the ratio between positive BSA-1 labeling area and whole tissue area was calculated as:

BSA-I stained area / whole tissue area.

2.9. Statistical analysis

To determine differences between infected and control group, Student's *t*-test was used. Results are shown as mean ± standard deviation (SD). Significance was assumed at values of $p < 0.05$.

3. Results

3.1. Clinical signs

Infected mice showed slight respiratory signs and ruffled fur during the first two days pi, without weight lost when compared to control mice. Although infected mice showed a reduced number of fetuses differences were not statistically significant.

3.2. Virus isolation, PCR and immunohistochemical antigen detection

Virus isolation and DNA detection was positive in the lungs of the infected mice at days 3 and 4 pi, but negative in uteri, placental units, livers and spleens. Viral antigens were only detected by immunohistochemistry in bronchial and bronchiolar epithelia in both infected groups (Fig. 2B).

3.3. Histological findings

Lungs, placentas and fetuses of control mice showed normal histological characteristics. Lungs of infected mice showed mild lymphocytic infiltration surrounding respiratory airways and infection foci at distal bronchial or bronchiolar epithelia (Fig. 2A). No gross abnormalities were observed in liver, spleen or central nervous system. Placentas of infected mice showed general vascular congestion in the labyrinth,

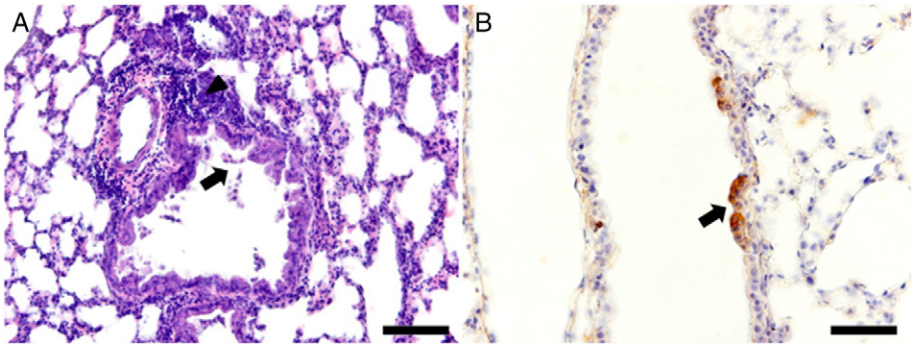

Fig. 2. A. Histological aspect of lungs from animals inoculated with the AR8 strain and isolated on day 3 pi. The arrow shows detachment of the bronchiolar epithelium, and the arrow head shows moderate mononuclear infiltration around airways and vessels, changes indicative of infection. HE staining. Bar = 100 μm. B. Immunohistochemical labeling of EHV-1 antigen in bronchiolar epithelial cells (arrow). Bar = 50 μm.

occasional thrombi in small vessels of spongiotrophoblast layers and decidua (Fig. 3A-B). In addition, in some placentas of both infected groups a reduction of the spongiotrophoblast zone with tracts of necrosis and a great number of uNK cells were found (Fig. 3C–D).

3.4. Morphometry

3.4.1. Spongiotrophoblast and labyrinth areas

An increase in the labyrinth area of both infected groups was observed, but it was only significant in mice of the ID3 group. The area of the spongiotrophoblast showed a significant reduction by day 3 pi but an increase by day 4pi (Fig. 4).

3.4.2. Proliferation and cell death assessment

Proliferation was significantly reduced in both infected groups whereas there was a significant increase in the apoptosis in comparison to their corresponding control groups (Fig. 5).

3.4.3. BSA-I lectin labeling

The stained area corresponding to fetal capillary endothelium surface was significantly reduced in both infected groups (Fig. 6).

3.5. Cytokine determination

The relative quantification of the cytokines studied by qPCR showed a significant increase in the IL-10 mRNA of the placentas of all infected mice, and in the uteri of the ID3 group. TNF-α mRNA was significantly decreased in the placentas of the ID3 mice whereas there was an increase in the uteri of the ID4 group. On the other hand, INF-γ mRNA significantly decreased in the placentas of both infected groups, but it increased in their uteri (Fig. 7).

The expression of TNF-α, IFN-γ and IL-10 proteins were corroborated by flow cytometry. TNF-α was significantly increased at day 3 pi in the placentas and uteri with respect to control group. No significant differences were found for IFN-γ and IL-10 (Fig. 8).

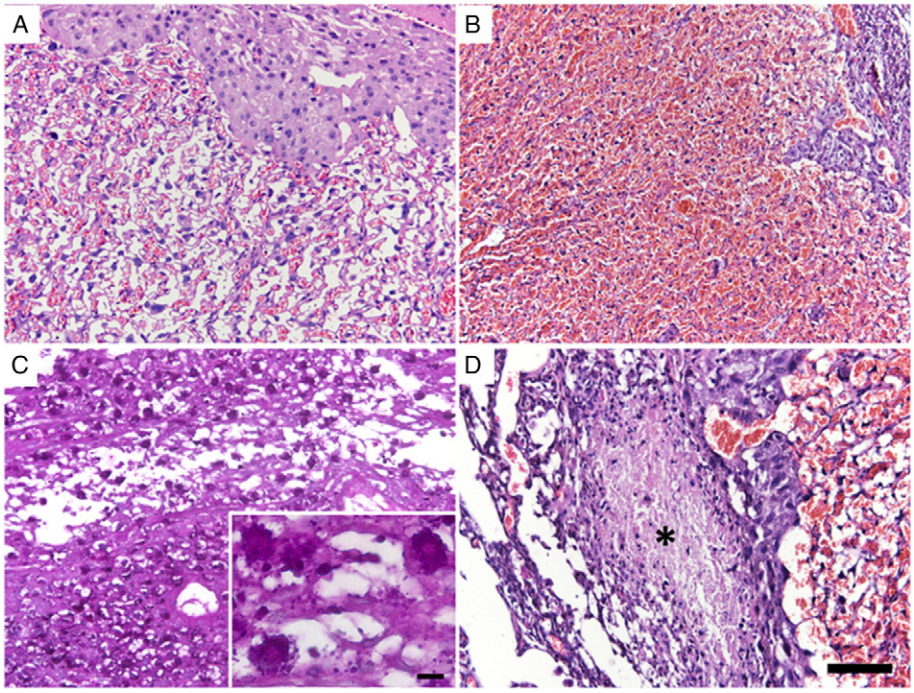

Fig. 3. Histological aspects of the placenta. A. Control placenta. B. Infected placenta (ID4 group) showing vascular congestion in the labyrinth zone. HE staining. C. uNK cells in spongiotrophoblast and decidua of infected mice. Inset: detail of uNK cell. PAS technique (arrows) D. Necrotic areas in the spongiotrophoblast zone (*). HE staining. Bar = 100 μm for A–D; inset bar = 10 μm.

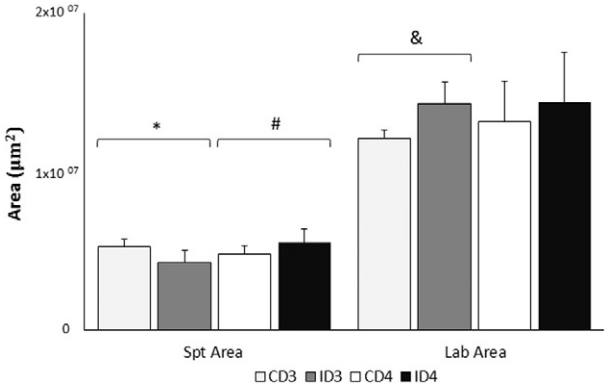

Fig. 4. Morphometry of spongiotrophoblast and labyrinth areas. Significant increase in the labyrinth area of infected mice at day 3 pi (&), $p < 0.05$. Spongiotrophoblast area showed a significant reduction by day 3 pi (*), and an increase by day 4 (#), $p < 0.05$.

4. Discussion

Here we provided a description of placental changes observed in the murine model during EHV-1 infection, including aspects that have not yet been fully investigated, such as variations on local cytokine expression, and processes such as cell proliferation and death which, to our knowledge, have not been investigated before in EHV infected mice.

Descriptions of the effects of EHV-1 strains at different stages of pregnancy using the murine model have been made by several authors (Awan et al., 1991, 1995; Inazu et al., 1993; Iwai et al., 1998; Walker et al., 1999a, 1999b; Smith et al., 2000). Here, we reported vascular changes, as it has been reported by Walker et al. (1999a, 1999b) in mice, and by Allen and Bryans (1986) in mares, and a reduction in the endothelial vascular area of the labyrinth by using BSA-1 lectin, which has not been reported before and may be secondary to the congestion. The increase in the labyrinth area may be due to vascular congestion here reported. Spongiotrophoblast area reduction may be explained by the necrosis produced as a consequence of congestion, which was less evident by day 4 pi. Onset and severity of clinical signs vary with the dose and strain of virus used to inoculate mice (Walker et al., 1999b). The clinical signs here reported were not as severe as those present after the intranasal inoculation of AB4 and 1939 strains at mid-gestation, which also caused the abortion of infected offsprings (Awan et al., 1991). However, similar lesions to those here described were reported by Walker et al. (1999a) after the intranasal inoculation of the abortigenic HVS25A strain, and by Iwai et al. (1998) with the HH1 strain, although mice infected with the latter strain displayed more evident signs. On the other hand, adult mice inoculated with the 1939 strain showed no clinical signs and gave birth to dead or malformed offsprings (Awan et al., 1991). Few researchers could detect viral antigens in lungs, liver, and placental and fetal tissues (Awan et al., 1995). In our study mice were euthanized before natural parturition or abortion occurred and we could neither recover viral particles from the placentas nor detect viral DNA or antigens. However, we detected viral DNA and antigens in the infected lungs. It has been suggested that trophoblasts infected by EHV-1 (Mukaiya et al., 2000) or by the neurotrophic EHV-9, which shares serological characteristics with EHV-1 and also induces abortion (El-Habashi et al., 2011), may suppress or limit virus replication, a fact that might explain the difficulty to detect viral antigens in the tissues. As it comes out, results might vary between the experiments carried out and it is difficult to compare them. Most of these studies were developed using experimental designs that varied on doses, via and days of pregnancy selected for the virus inoculation, as well as in the pi time points analyzed.

Cell proliferation and death occur cyclically in the uterus and placenta under physiological conditions (Joswig et al., 2003), but they may be altered by several non-infectious and infectious states. In the infected placentas we found a reduction in cell proliferation and an increase in the apoptosis. In other pathologies in which uteroplacental ischemia occurs (Gül et al., 2015), placentas showed a significant increase in apoptosis and proliferation, the latter as a compensatory response. Here, we infer that placentas from infected mice are indeed ischemic; however, in our model proliferation decreased, maybe because the time was insufficient for the cell to proliferate. The increase in apoptosis may be used by the virus to enhance the efficient diffusion of its progeny to neighboring cells, such as macrophages (Pagnini et al., 2005; Longo et al., 2009).

Many aspects of the *in vivo* and *in vitro* immune response to EHV-1 infection in the natural host as well as in the experimental murine model need to be explored. We investigated for the first time whether the local expression of IFN-γ, TNF-α and IL-10 is altered in mice uteri and placentas, changes that may also occur in pregnant mares. The IFNs are a large family of multifunctional secreted proteins involved in the activation of the innate and adaptive immune system, cell proliferation and apoptosis (Mor and Cardenas, 2010). Particularly, IFN-γ, a type II IFN, is synthesized once infected cells are recognized by activated T lymphocytes and NK cells, and it is crucial for the activation of adaptive immune responses against different pathogens. In the present study we found an increase in mRNA of IFN-γ, in the uteri of infected mice, which may be understood as a response to the infection state. In contrast, opposite results were found in the infected placentas. It is known that trophoblast cells have developed mechanisms to block IFN-γ signaling in order to contribute to a successful pregnancy by avoiding fetal rejection (Murphy et al., 2009). In addition, interferons and other antiviral cytokines are synthetized by trophoblast cells in response to viral infections, as a mechanism to prevent the virus arrival to the placenta and fetus (Mor and Cardenas, 2010). On the other hand, many viruses have developed different evasive mechanisms to interfere with the IFN-γ function at different levels of the signaling pathway of this cytokine (Goodbourn et al., 2000; Haller et al., 2006; Sarkar et al., 2015). Nevertheless, it is unknown whether the low placenta IFN-γ level may be explained by the existence of an evasive mechanism of EHV-1 AR8-strain or the by a

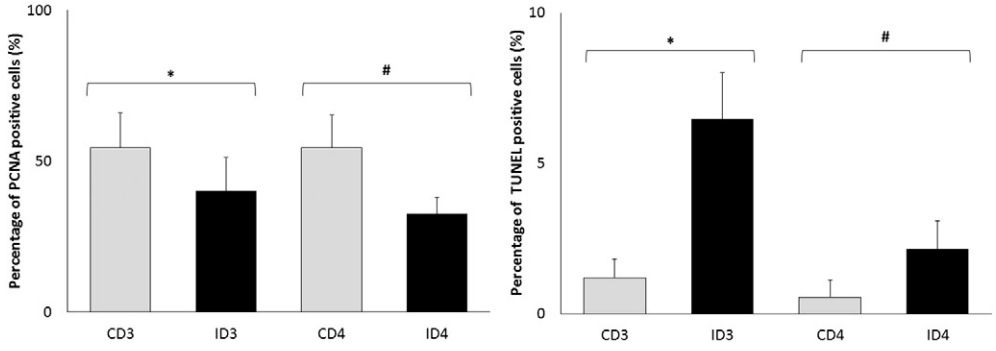

Fig. 5. Proliferation and cell death assessment. Proliferation (PCNA determination) was significantly reduced in both infected groups (*, #), whereas apoptosis (TUNEL determination) was significantly increased (*, #), $p < 0.05$.

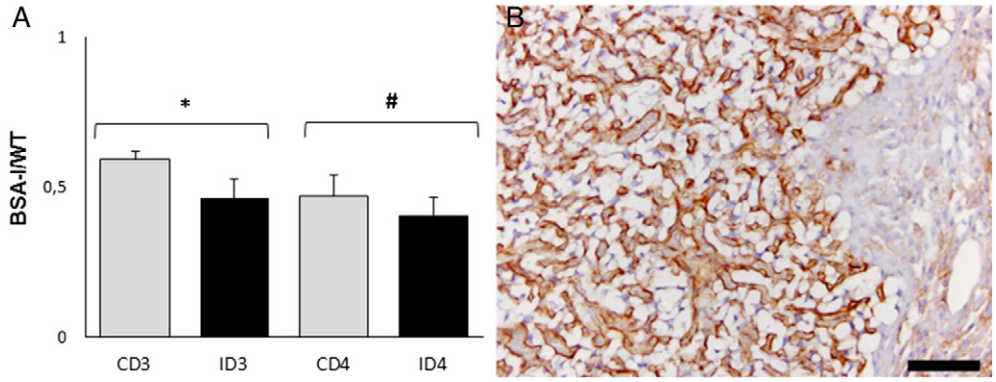

Fig. 6. BSA-I lectin labeling in the placentas of infected mice. A. Significant reduction of the stained area corresponding to fetal endothelial capillaries surface in both infected groups (ID3 -*- and ID4 -&-), $p < 0.05$. B. BSA-1 labeling in the placenta of infected mice at day 4 pi. WT: whole tissue. Bar = 50 μm.

protective effect exerted by trophoblast to prevent the infection of placenta and fetus.

TNF is a pro-inflammatory cytokine that regulates different cellular processes during normal pregnancy, such as cell proliferation, differentiation and apoptosis (Haider and Knöfler, 2009). Nevertheless, it also induces adverse effects for pregnancy, and it is implicated in the pathogenesis of several reproductive disorders, depending on its concentrations, distribution of TNF receptors, length of TNF stimulation and the cell types involved (Haider and Knöfler, 2009; Azizieh and Raghupathy, 2015). As it was observed for IFN-γ, here we found a mRNA down-regulation of TNF in the infected placentas but higher protein levels, possibly from a systemic origin. In contrast, in the uteri we found a normal response to the infection with an increase in TNF at both transcriptional and translational levels.

IL10 has protective effects during pregnancy, since it inhibits the secretion of inflammatory cytokines, such as TNF and IFN-γ and therefore, it contributes to a normal pregnancy development (Brogin Moreli et al., 2012). Here, we observed an up-regulation of this cytokine in the placentas and uteri of infected mice. The expression of IL10 under EHV-1 infection may be exacerbated to further protect the organ from inflammation and to restore the immunological homeostasis. However, it is also worthy to mention that during certain viral infections IL10 has a

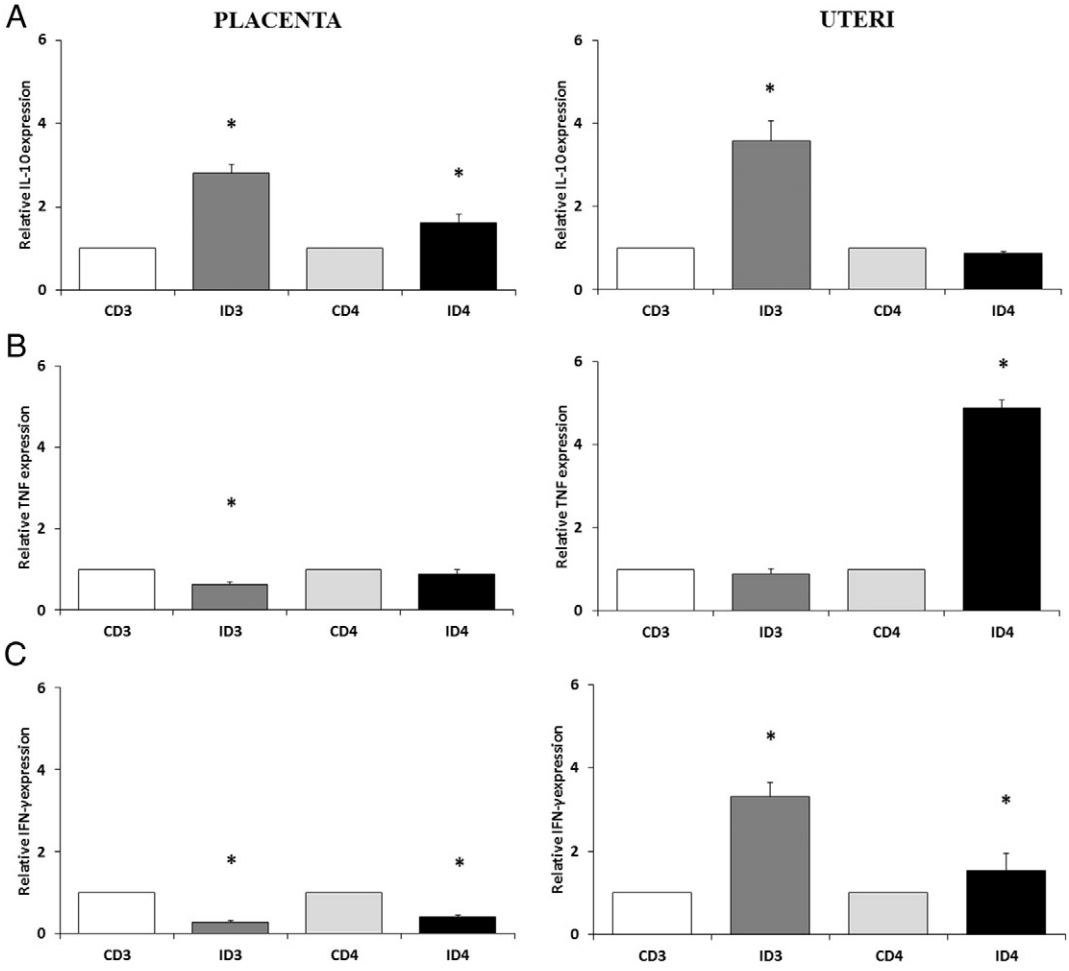

Fig. 7. Transcripts of TNF-α, IFN-γ and IL-10 were determined by qRT-PCR in placentas and uteri of control and infected mice. (*) Significant differences with its own time control, $p < 0.05$.

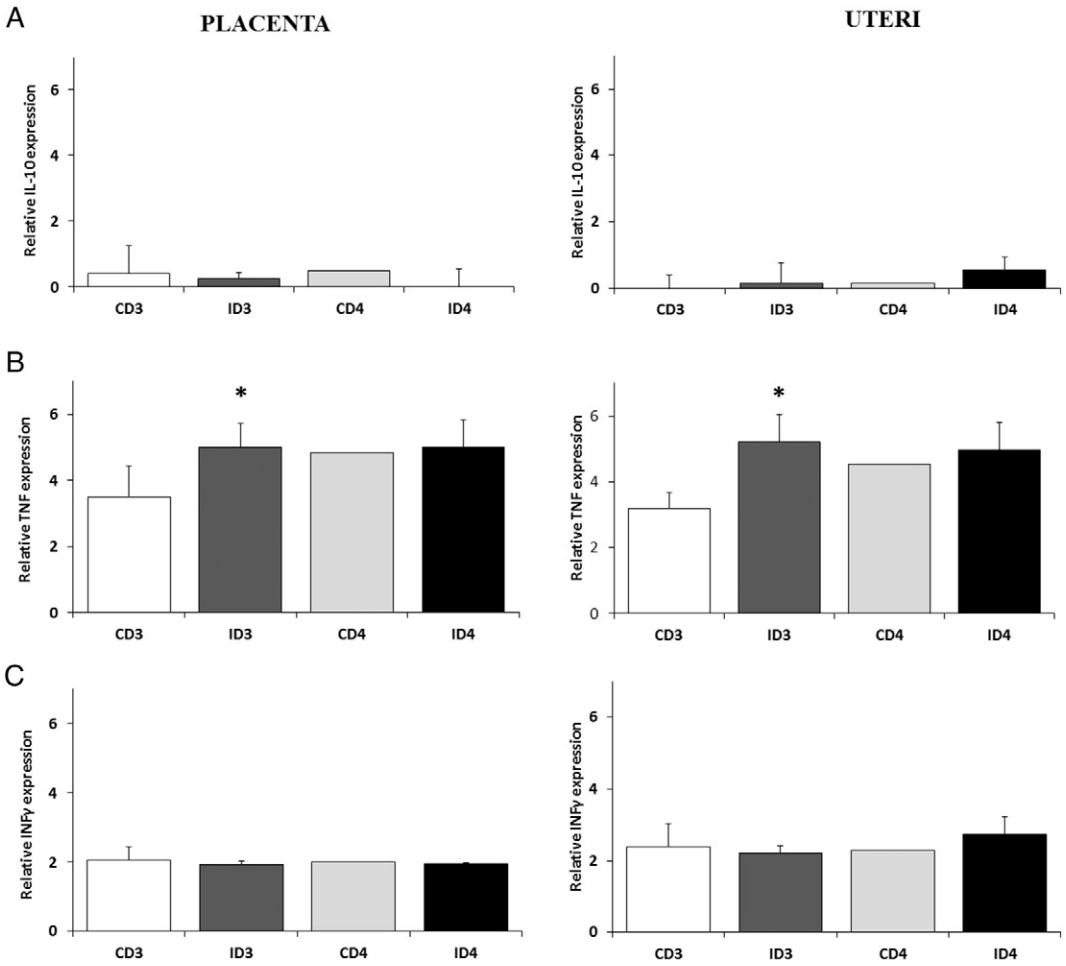

Fig. 8. Flow cytometry of TNF-α, IFN-γ and IL-10 proteins in placentas and uteri of control and infected mice. (*) Significant differences with its own time control, $p < 0.05$.

different role. Indeed, IL10 is involved in the establishment and perpetuation of viral persistence. Viruses that generate latent infection, such as EHV-1, may encode their own IL-10 homologs to modulate the immune response and facilitate its replication, spread and/or persistence (Wilson and Brooks, 2011).

Several alphaherpesvirus are able to control the host immune response by blocking or modulating the expression of antiviral cytokines (Paladino and Mossman, 2009). Sarkar et al. (2015) showed that the T953 EHV-1 strain, isolated from a horse suffering a neurological disease, suppresses the antiviral type-1-IFN response in vitro, being in agreement with our results regarding IFN. Wagner et al. (2011) compared in vitro the effects of a neuropathogenic and two abortigenic EHV-1 strains on IL10, IL4 and IFN-α expression using peripheral blood mononuclear cells (PBMC) from foals, pregnant and non-pregnant mares, and found that IFN-α expression was similarly up-regulated by the three strains in all cell cultures. Wimer et al. (2011) also reported similar induction of IFN-α by two abortigenic and one neuropathogenic strain in equine PBMC. Here we found a decrease in IFN-γ expression using an abortigenic strain. As it can be analyzed, most of the results were obtained in vitro and there is no general consensus of the effects of EHV-1 on the cytokine expression, since the response varies with the virus strain and the experimental cell lines used. On the other hand, in the in vivo model the immunological mechanisms involved are much complex, due to the contribution and interplay of different cell types and extracellular components. Pusterla et al. (2006) could not detect IL-10 and IFN-γ transcripts in brain and spinal cord tissues of horses infected by EHV-1. It remains unknown whether the ability to control the immune response in one way or another occurs always in vivo with all the neuropathogenic or abortigenic strains.

Although most of these changes may be specifically induced by the virus, it is known that variations in placental cytokine production also occur following changes in the oxygen tension (Benyo et al., 1997; Royle et al., 2009). The vascular congestion present in the infected placentas reduces the normal oxygen tension, and consequently, may also affect the local synthesis, secretion and regulation of cytokines.

5. Conclusions

We conclude that the effects of EHV-1 during pregnancy depend on different pathogenic mechanisms in which vascular, cell death and proliferation changes and local cytokine expression are involved. Future studies will include the investigation of the role of uNK cells and other immune cells in the regulation of these changes.

The understanding of the immunological impact of systemic and local EHV-1 infection in the murine model will help to address future studies in the horse to improve the prophylactic and therapeutic strategies to protect this species from reproductive failures.

Conflict of interest statement

There are no conflicts of interest regarding authorship or publication of this article.

Acknowledgments

This study was supported by grants from the National Agency of Science and Technology (BID PICT 2011-1123), *Scientific Research Commission* of Province of Buenos Aires, Argentina (CIC-PBA) (1376/12 and 1395/13), the Department for Science and Technology of the National University of La Plata (Projects 11-V188 and 11-V221). We also thank Mrs. Rosa Villegas, Mrs. Guadalupe Guidi, Mr. Rubén Mario, Mr. Claudio A. Leguizamón and Mrs. Adriana Conde for their technical support.

References

Allen, G.P., Bryans, J.T., 1986. Molecular epizootiology, pathogenesis and prophylaxis of equine herpesvirus-1 infections. In: Pandey, R. (Ed.), Progress in Veterinary Microbiology and Immunology. Karger, Basel, pp. 78–144.

Awan, A.R., Gibson, J.S., Field, H.J., 1991. A murine model for studying EVH-1-induced abortion. Res. Vet. Sci. 51, 94–99.

Awan, A.R., Baxi, M., Field, H.J., 1995. EHV-1 induced abortion in mice and its relationship to stage of gestation. Res. Vet. Sci. 59, 139–145.

Azizieh, F.Y., Raghupathy, R.G., 2015. Tumor necrosis factor-α and pregnancy complications: a prospective study. Med. Princ. Pract. 24, 165–170.

Bancroft, J.D., Stevens, A., 1990. Theory and Practice of Histological Techniques. Churchill Livingstone, Edinburgh.

Benyo, D.F., Miles, T.M., Conrad, K.P., 1997. Hypoxia stimulates cytokine production by villous explants from the human placenta. J. Clin. Endocrinol. Metab. 82, 1582–1588.

Bilinski, M.J., Thorne, J.G., Oh, M.J., Leonard, S., Murrant, C., Tayade, C., Croy, B.A., 2008. Uterine NK cells in murine pregnancy. Reprod. BioMed. Online 16, 218–226.

Brogin Moreli, J., Cirino Ruocco, A.M., Vernini, J.M., Rudge, M.V., Calderon, I.M., 2012. Interleukin 10 and tumor necrosis factor-alpha in pregnancy: aspects of interest in clinical obstetrics. ISRN Obstet. Gynecol. 2012, 230742.

Bulmer, J.N., Lash, G.,.E., 2015. The role of uterine NK cells in normal reproduction and reproductive disorders. Adv. Exp. Med. Biol. 868, 95–126.

Charalambous, C., Drakou, K., Nicolaou, S., Georgiades, P., 2013. Novel spatiotemporal glycome changes in the murine placenta during placentation based on BS-I lectin binding patterns. Anat. Rec. 296, 921–932.

de la Fuente, R., Awan, A.R., Field, H.J., 1992. The acyclic nucleoside analogue penciclovir is a potent inhibitor of equine herpesvirus type 1 (EHV-1) in tissue culture and in a murine model. Antivir. Res. 18, 77–89.

El-Habashi, N., El-Nahass, E., Fukushi, H., Nayel, M., Hibi, D., Sakai, H., Yanai, T., 2011. Effects of equine herpesvirus-9 infection in pregnant mice and hamsters. J. Comp. Pathol. 144, 103–112.

Fitzmaurice, T., Walker, C., Kukreja, A., Sun, Y., Brown, S.M., Field, H.J., 1997. The pathogenesis of ED71, a defined deletion mutant of equine herpesvirus-1, in a murine intranasal infection model for equine abortion. J. Gen. Virol. 78, 2167–2169.

Fuentealba, N.A., Sguazza, G.H., Eöry, M.L., Valera, A.R., Pecoraro, M.R., Galosi, C.M., 2011. Genomic study of Argentinean Equid herpesvirus 1 strains. Rev. Argent. Microbiol. 43, 273–277.

Fuentealba, N.A., Zanuzzi, C.N., Scrochi, M.R., Sguazza, G.H., Bravi, M.E., Cid de la Paz, V., Corva, S.G., Portiansky, E.L., Gimeno, E.J., Barbeito, C.G., Galosi, C.M., 2014. Protective effects of intranasal immunization with recombinant glycoprotein d in pregnant BALB/c mice challenged with different strains of equine herpesvirus 1. J. Comp. Pathol. 151, 384–393.

Galosi, C.M., Vila Roza, M.V., Oliva, G.A., Pecoraro, M.R., Echeverría, M.G., Corva, S., Etcheverrigaray, M.E., 2001. A polymerase chain reaction for detection of equine herpesvirus-1 in routine diagnostic submissions of tissues from aborted foetuses. J. Vet. Med. B Infect. Dis Vet. Public Health 48, 341–346.

Goodbourn, S., Didcock, L., Randall, R.E., 2000. Interferons: cell signalling, immune modulation, antiviral response and virus countermeasures. J. Gen. Virol. 81, 2341–2364.

Gül, M., Bayat, N., Çetin, A., Kepekçi, R.A., Şimşek, Y., Kayhan, B., Turhan, U., Otlu, A., 2015. Histopathological, ultrastructural and apoptotic changes in diabetic rat placenta. Balkan Med. J. 32, 296–302.

Haider, S., Knöfler, M., 2009. Human tumour necrosis factor: physiological and pathological roles in placenta and endometrium. Placenta 30, 111–123.

Haller, O., Kochs, G., Weber, F., 2006. The interferon response circuit: induction and suppression by pathogenic viruses. Virology 344, 119–130.

Inazu, M., Tsuha, O., Kirisawa, R., Kawakami, Y., Iwai, H., 1993. Equid herpesvirus 1 infection in mice. J. Vet. Med. Sci. 55, 119–121.

Iwai, H., Kodera, A., Noriyuki, S., Nakamura, A., 1998. Effect of equid herpesvirus 1 infection on parturition of mice. J. Equine. Sci. 9, 25–27.

Joswig, A., Gabriel, H.D., Kibschull, M., Winterhager, E., 2003. Apoptosis in uterine epithelium and decidua in response to implantation: evidence for two different pathways. Reprod. Biol. Endocrinol. 26, 1–44.

Kusakabe, K., Okada, T., Sasaki, F., Kiso, Y., 1999. Cell death of uterine natural killer cells in murine placenta during placentation and preterm periods. J. Vet. Med. Sci. 61, 1093–1100.

Lash, G.E., Bulmer, J.N., 2011. Do uterine natural killer (uNK) cells contribute to female reproductive disorders? J. Reprod. Immunol. 88, 156–164.

Longo, M., Fiorito, F., Marfè, G., Montagnaro, S., Pisanelli, G., De Martino, L.G., Iovane, G., Pagnini, U., 2009. Analysis of apoptosis induced by caprine Herpesvirus1 *in vitro*. Virus Res. 145, 227–235.

Lunn, D.P., Davis-Poynter, N., Flaminio, M.J., Horohov, D.W., Osterrieder, K., Pusterla, N., Townsend, H.G., 2009. Equine herpesvirus-1 consensus statement. J. Vet. Intern. Med. 23, 450–461.

Mor, G., Cardenas, I., 2010. The immune system in pregnancy: a unique complexity. Am. J. Reprod. Immunol. 63, 425–433.

Motta, C., Grosso, C., Zanuzzi, C., Molinero, D., Picco, N., Bellingeri, R., Alustiza, F., Barbeito, C., Vivas, A., Romanini, M.C., 2015. Effect of sildenafil on pre-eclampsia-like mouse model induced by L-name. Reprod. Domest. Anim. 50, 611–616.

Mukaiya, R., Kimura, T., Ochiai, K., Wada, R., Umemura, T., 2000. Demonstration of equine herpesvirus-1 gene expression in the placental trophoblasts of naturally aborted equine fetuses. J. Comp. Pathol. 123, 119–125.

Murphy, S.P., Tayade, C., Ashkar, A.A., Hatta, K., Zhang, J., Croy, B.C., 2009. Interferon gamma in successful pregnancies. Biol. Reprod. 80, 848–859.

Osterrieder, N., Neubauer, A., Brandmüller, C., Kaaden, O.R., O'Callaghan, D.J., 1996. The equine herpesvirus 1 IR6 protein influences virus growth at elevated temperature and is a major determinant of virulence. Virology 226, 243–251.

Pagnini, U., Montagnaro, S., Sanfelice di Monteforte, E., Pacelli, F., De Martino, L., Roperto, L., Florio, S., Iovane, G., 2005. Caprine herpesvirus-1 (CapHV-1) induces apoptosis in goat peripheral blood mononuclear cells. Vet. Immunol. Immunopathol. 103, 283–293.

Paladino, P., Mossman, K.L., 2009. Mechanisms employed by herpes simplex virus 1 to inhibit the interferon response. J. Interf. Cytokine Res. 29, 599–607.

Pusterla, N., Wilson, W.D., Conrad, P.A., Barr, B.C., Ferraro, G.L., Daft, B.M., Leutenegger, C.M., 2006. Cytokine gene signatures in neural tissue of horses with equine protozoal myeloencephalitis or equine herpes type 1 myeloencephalopathy. Vet. Rec. 159, 341–346.

Royle, C., Lim, S., Xu, B., Tooher, J., Ogle, R., Hennessy, A., 2009. Effect of hypoxia and exogenous IL-10 on the pro-inflammatory cytokine TNF-alpha and the anti-angiogenic molecule soluble Flt-1 in placental villous explants. Cytokine 47, 56–60.

Ruitenberg, K.M., Walker, C., Wellington, J.E., Love, D.N., Whalley, J.M., 1999. DNA-mediated immunization with glycoprotein D of equine herpesvirus 1 (EHV-1) in a murine model of EHV-1 respiratory infection. Vaccine 21, 237–244.

Sarkar, S., Balasuriya, U.B., Horohov, D.W., Chambers, T.M., 2015. Vet. Immunol. Immunopathol. 167, 122–129.

Smith, K.C., Whitwell, K.E., Mumford, J.A., Hannant, D., Blunden, A.S., Tearle, J.P., 2000. Virulence of the V592 isolate of equid herpesvirus-1 in ponies. J. Comp. Pathol. 122, 288–297.

Wagner, B., Wimer, C., Osterrieder, N., Erb, H.N., 2011. Infection of peripheral blood mononuclear cells with neuropathogenic equine herpesvirus type-1 strain Ab4 reveals intact interferon-α induction and induces suppression of anti-inflammatory interleukin-10 responses in comparison to other viral strains. Vet. Immunol. Immunopathol 143, 116–124.

van Woensel, P.A., Goovaerts, D., Markx, D., Visser, N., 1995. A mouse model for testing the pathogenicity of equine herpes virus-1 strains. J. Virol. Methods 54, 39–49.

Walker, C., Perotti, V.M., Love, D.N., Whalley, J.M., 1999a. Infection with equine herpesvirus 1 (EHV-1) strain HVS25A in pregnant mice. J. Comp. Pathol. 120, 15–27.

Walker, C., Love, D.N., Whalley, J.M., 1999b. Comparison of the pathogenesis of acute equine herpesvirus 1 (EHV-1) infection in the horse and the mouse model: a review. Vet. Microbiol. 68, 3–13.

Whitten, W.K., 1966. Pheromones and mammalian reproduction. Adv. Reprod. Physiol. 155-177.

Wilson, E.B., Brooks, D.G., 2011. The role of IL-10 in regulating immunity to persistent viral infections. Curr. Top. Microbiol. Immunol. 350, 39–65.

Wimer, C.L., Damiani, A., Osterrieder, N., Wagner, B., 2011. Equine herpesvirus type-1 modulates CCL2, CCL3, CCL5, CXCL9, and CXCL10 chemokine expression. Vet. Immunol. Immunopathol. 140, 266–274.

Woudwyk, M.A., Monteavaro, C.E., Jensen, F., Soto, P., Barbeito, C.G., Zenclussen, A.C., 2012. Study of the uterine local immune response in a murine model of embryonic death due to *Tritrichomonas foetus*. Am. J. Reprod. Immunol. 68, 128–137.

Woudwyk, M.A., Gimeno, E.J., Soto, P., Barbeito, C.G., Monteavaro, C.E., 2013. Lectin binding pattern in the uterus of pregnant mice infected with *Tritrichomonas foetus*. J. Comp. Pathol. 149, 341–345.

Zanuzzi, C., Scrochi, M., Fuentealba, N., Nishida, F., Portiansky, E., Muglia, C., Gimeno, E., Barbeito, C., Galosi, C., 2014. Effects of equid herpesvirus 1 (EHV-1) AR8 and HH1 strains on BALB-c mice. Arch. Virol. 159, 141–145.

Zhang, Y., Smith, P.M., Jennings, S.R., O'Callaghan, D.J., 2000. Quantitation of virus-specific classes of antibodies following immunization of mice with attenuated equine herpesvirus 1 and viral glycoprotein D. Virology 268, 482–492.